Systems/Circuits

Distinctive Modulation of Dopamine Release in the Nucleus Accumbens Shell Mediated by Dopamine and Acetylcholine Receptors

Jung Hoon Shin,* Martin F. Adrover,* and Veronica A. Alvarez

Laboratory on Neurobiology of Compulsive Behaviors, National Institute on Alcohol Abuse and Alcoholism, National Institutes of Health, Bethesda, Maryland 20892

Nucleus accumbens (NAc) shell shows unique dopamine (DA) signals *in vivo* and plays a unique role in DA-dependent behaviors such as reward-motivated learning and the response to drugs of abuse. A disynaptic mechanism for DA release was reported and shown to require synchronized firing of cholinergic interneurons (CINs) and activation of nicotinic acetylcholine (ACh) receptors (nAChRs) in DA neuron (DAN) axons. The properties of this disynaptic mechanism of DA transmission are not well understood in the NAc shell. In this study, *in vitro* fast-scan cyclic voltammetry was used to examine the modulation of DA transmission evoked by CINs firing in the shell of mice and compared with other striatal regions. We found that DA signals in the shell displayed significant degree of summation in response to train stimulation of CINs, contrary to core and dorsal striatum. The summation was amplified by a D2-like receptor antagonist and experiments with mice with targeted deletion of D2 receptors to DANs or CINs revealed that D2 receptors in CINs mediate a fast inhibition observed within 100 ms of the first pulse, whereas D2 autoreceptors in DAN terminals are engaged in a slower inhibition that peaks at ~500 ms. ACh also contributes to the use-dependent inhibition of DA release through muscarinic receptors only in the shell, where higher activity of acetylcholinesterase minimizes nAChR desensitization and promotes summation. These findings show that DA signals are modulated differentially by endogenous DA and ACh in the shell, which may underlie the unique features of shell DA signals *in vivo*.

Key words: **D2 receptors; G-protein coupled receptors; muscarinic receptors; nicotinic receptors; optogenetics; voltammetry**

Significance Statement

The present study reports that dopamine (DA) release evoked by activation of cholinergic interneurons displays a high degree of summation in the shell and shows unique modulation by endogenous DA and acetylcholine. Desensitization of nicotinic receptors, which is a prevailing mechanism for use-dependent inhibition in the nucleus accumbens core and dorsal striatum, is also minimal in the shell in part due to elevated acetylcholinesterase activity. This distinctive modulation of DA transmission in the shell may have functional implications in the acquisition of reward-motivated behaviors and reward seeking.

Introduction

The shell is the most ventral part of nucleus accumbens (NAc) and has unique anatomical features that define a separate circuitry within the basal ganglia (Humphries and Prescott, 2010). The shell receives inputs from limbic structures (Lu et al., 1998; Zhou et al., 2003; Britt et al., 2012) and also projects widely outside of the basal ganglia, including to lateral hypothalamus, pedunculopontine nucleus, and thalamus, but not to substantia nigra or subthalamic nucleus (Mogenson et al., 1985; Yang and Mogenson, 1987; Groenewegen et al., 1993; Lavín and Grace, 1994; Pennartz et al., 1994). The NAc shell encodes specific aspects of reward processing such as context and cue information (Bossert et al., 2007; West and Carelli, 2016) and it is critical in mediating reinforcing and rewarding properties of stimulant drugs (McBride et al., 1999; Kelley, 2004; Wise, 2004; Everitt and Robbins, 2005; Crombag et al., 2008).

Collective evidence from *in vivo* studies suggest that dopamine (DA) transmission in the NAc shell is regulated differen-

Received March 2, 2017; revised Sept. 29, 2017; accepted Oct. 6, 2017.

Author contributions: J.H.S., M.F.A., and V.A.A. designed research; J.H.S. and M.F.A. performed research; J.H.S. and M.F.A. analyzed data; J.H.S., M.F.A., and V.A.A. wrote the paper.

This work was funded by the Intramural Programs of National Institute on Alcohol Abuse and Alcoholism and National Institute of Neurological Disorders and Stroke (Grant ZIA-AA000421). We thank Roland Bock (National Institute on Alcohol Abuse and Alcoholism–National Institutes of Health) for developing the analysis software and David Lovinger and the members of the Alvarez laboratory for valuable comments on this manuscript.

The authors declare no competing financial interests.

*J.H.S. and M.F.A. contributed equally to this work.

Correspondence should be addressed to Dr. Veronica A. Alvarez, National Institute on Alcohol Abuse and Alcoholism, National Institutes of Health, 5625 Fishers Lane, Bethesda, MD 20892. E-mail: alvarezva@mail.nih.gov.

DOI:10.1523/JNEUROSCI.0596-17.2017

 0270-6474/17/3711166-15$15.00/0

tially by D2/3 receptors to give rise to larger increase of DA levels upon cocaine exposure than in other regions (Jones et al., 1996; Di Chiara and Bassareo, 2007; Aragona et al., 2008; Aragona et al., 2009; Dreyer et al., 2016). Furthermore, antipsychotic drugs, mostly D2/3 receptor antagonists, produce larger increases of DA concentration in the NAc shell compared with core and prefrontal cortex (Tanda et al., 2015). The properties of DA release *in vitro* have been studied in the shell using electrical stimulation and modulation by acetylcholine (ACh) through the nicotinic ACh receptors (nAChRs) and muscarinic ACh receptors (mAChRs) has been proposed (Threlfell et al., 2010; Patel et al., 2012; Shin et al., 2015). However, DA release can be evoked in the striatum by different mechanisms: a monosynaptic mechanism that involves direct firing of action potentials in DA neuron (DAN) axons and by a disynaptic mechanism that requires synchronized firing of cholinergic interneurons (CINs) and activation of nAChRs on DAN axons (Cachope et al., 2012; Threlfell et al., 2012; Wang et al., 2014; Shin et al., 2015). These two mechanisms differ in the dependence of the DA response to the frequency of stimulation. For example, in the dorsal striatum, DA signals show summation in the amplitude of the DA signal in response to trains of stimulation when evoked by the monosynaptic but not by the disynaptic mechanism (Threlfell et al., 2012). This lack of summation is likely due to the inhibition of subsequent DA release during the train stimulation.

Desensitization of nAChRs has been suggested as a mechanism for the lack of summation of DA release evoked by train stimulation of CINs (Threlfell et al., 2012). nAChRs expressed in DAN axons contain β2-subunits and are highly prone to desensitization, which depends on the extracellular concentration of ACh (Giniatullin et al., 2005). The degree of nAChR desensitization is then in part regulated by the balance between release and clearance mechanisms for ACh. Acetylcholinestease, an extracellular enzyme for ACh degradation, has been shown to have a higher activity the NAc shell than other striatal subregions in several animal species (Záborszky et al., 1985; Voorn et al., 1994; Franklin and Paxinos, 2007). In this study, we explored whether acetylcholinestease activity regulates the degree of desensitization and if desensitization of nAChRs is less dominant in the NAc shell, rendering a different frequency summation in this region. $G_{i/o}$-protein coupled D2Rs and mAChRs in CINs (Yan and Surmeier, 1996; Yan et al., 1997; Alcantara et al., 2003) and DAN axons (Sesack et al., 1994) modulate the release of ACh and DA (Threlfell et al., 2010; Cachope et al., 2012; Adrover et al., 2014; Shin et al., 2015; Sulzer et al., 2016). We also explored whether these receptors are activated by endogenously released DA and ACh from previous activity and play a role in the inhibition of subsequent DA and ACh release in a use-dependent manner.

Materials and Methods

Animals. Heterozygote B6.SJL-*Slc6a3*$^{tm1.1(cre)Bkmn}$/J mice (006660; The Jackson Laboratory), referred to as DAT-cre mice; heterozygote B6N.129S6(B6)-*Chat*$^{tm2(cre)Lowl}$/J mice (018957; The Jackson Laboratory), referred as ChAT-cre mice; and the crosses of DAT-cre or ChAT-cre mice with B6.129S4(FVB)-*Drd2*$^{tm1.1Mrub}$/J mice (020631; The Jackson Laboratory), referred as autoDrd2KO mice (Bello et al., 2011) and CINDrd2KO mice (Kharkwal et al., 2016), respectively, were used for experiments. All mice were male in C57BL/6 background and housed on a 12 h light/dark cycle (06:30–18:30 light) with food and water *ad libitum*. All experiments were performed in accordance with guidelines from the National Institute on Alcohol Abuse and Alcoholism (NIAAA) Animal Care and Use Committee.

Stereotaxic injection of AAV-ChR2 vectors. Injections were performed as described previously Adrover et al. (2014). Briefly, mice (5–6 weeks old) anesthetized by a mixture of isoflurane-oxygen were placed in a stereotaxic frame (David Kopf). Adeno-associated virus (AAV) vectors carrying the sequence for Cre-dependent expression of Channelrhodopsin2 (ChR2) protein, AAV5-EF1a-DIO-hChR2(H134R)-EYFP (4×10^{12} IU/ml), were bilaterally injected into VTA/SNc (AP: −3.30, ML: ± 0.50, DV: −4.50) of DAT-cre or AutoDrd2KO mice or in the NAc (AP: +1.35, ML: ± 1.05, DV: −5.00) or dorsal striatum (AP: +1.05, ML: ± 1.20, DV: −3.20) of ChAT-cre or CINDrd2KO mice. All stereotaxic coordinates are in millimeters from bregma according to the atlas of Franklin and Paxinos (2007). The injection volumes were 300 nl at a flow rate of 100 nl/min. Recordings were made after a minimum of 3 weeks of incubation. Viral vectors were purchase from the Gene Therapy Center Vector Core at University of North Carolina.

Slice preparation. Brains were sliced in a vibratome (VT-1200S; Leica) in an ice-cold cutting solution containing the following (in mM): 225 sucrose, 13.9 NaCl, 26.2 $NaHCO_3$, 1 NaH_2PO_4, 1.25 glucose, 2.5 KCl, 0.1 $CaCl_2$, 4.9 $MgCl_2$, and 3 kynurenic acid. Sagittal slices (240 μm) were recovered for 20 min at 33°C in artificial CSF (ACSF) containing the following (in mM): 124 NaCl, 1 NaH_2PO_4, 2.5 KCl, 1.3 $MgCl_2$, 2.5 $CaCl_2$, 20 glucose, 26.2 $NaHCO_3$, and 0.4 ascorbic acid and were maintained in ACSF in the dark at room temperature prior recordings. Slices were recorded with continuous superperfusion (2 ml/min) of ACSF at 32°C using an inline heater (Harvard Apparatus).

Fast scan cyclic voltammetry (FSCV). Carbon fiber microelectrodes were prepared using a carbon fiber (7 μm diameter) inserted into a glass pipette (~150 μm of exposed fiber). The carbon-fiber microelectrode was held at −0.4 V versus Ag/AgCl and a triangular voltage ramp from −0.4 V to +1.2 V and back to −0.4 V (400 V/s) was delivered every 100 ms. DA transients were evoked by illuminating a brief (0.6 ms) light pulse using an optical fiber (200 μm/0.22 NA) connected to a 470 nm LED (2 mW; ThorLabs). The light pulses were delivered every 2 min. Data were collected with a retrofitted head stage (CB-7B/EC with 5 MΩ resistor) using a Multiclamp 700B amplifier (Molecular Devices), with digitization at 100 kHz using pClamp10 software (Molecular Devices) or using custom-written software in Igor Pro (Wavemetrics) running mafPC (courtesy of M.A. Xu-Friedman). All data collected were analyzed with the custom-written software. The current peak amplitudes of the evoked DA transients were converted to DA concentrations according to the postexperimental calibration using 1–3 μM DA. FSCV was performed in the NAc shell, NAc core, and dorsal striatum regions.

Cell-attached recording. Cell-attached recording was performed using glass pipettes (~4 MΩ) filled with Cs-based internal saline (Adrover et al., 2014). CINs from ChAT-cre mice infected with AAV5-EF1a-DIO-hChR2(H134R)-EYFP vector were identified with fluorescence and confirmed by their characteristic spontaneous firing pattern. The recordings were performed at holding potential of 0 mV with digitization at 5 kHz using pClamp10 software. Action potentials were evoked using the same light stimulation used to evoke DA transients (see above).

Drugs. Sulpiride, dihydro-β-erythroidine hydrobromide (DHβE), scopolamine, and ambenonium were purchased from Tocris Bioscience. Kynurenic acid (sodium salt) was obtained from Ascent Scientific. All other chemicals were from Sigma-Aldrich.

Experimental design and statistical analysis. For each dataset, recordings were made from at least five slices or cells derived from a total of at least three animals. Statistical analysis was performed with Prism software (GraphPad) using linear regression, unpaired two-tailed Student's *t* test, and one- and two-way ANOVA. Tukey's or Bonferroni's test for multiple comparisons were used for *post hoc* analysis.

Results

Frequency-dependent summation of DA signals in the shell region

To study the use-dependent modulation of DA release evoked by activation of CINs (Cachope et al., 2012; Threlfell et al., 2012), ChR2-EYFP was expressed in CINs in the NAc (Fig. 1*A*) and the dorsal striatum regions of ChAT-cre mice by bilateral local ad-

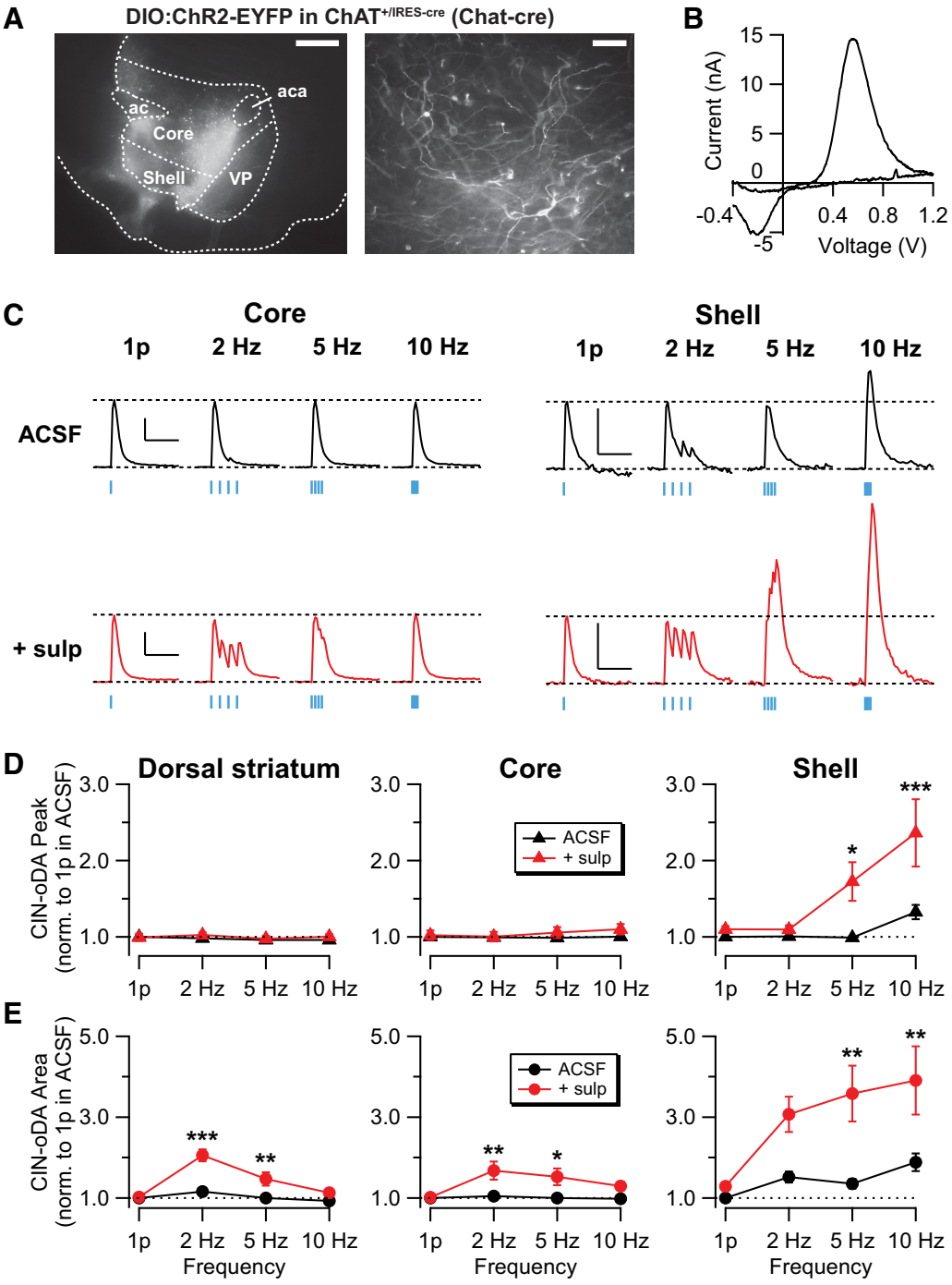

Figure 1. DA release evoked by optogenetic stimulation of CIN shows a frequency-dependent summation only in the NAc shell region of the striatum in the presence of D2 receptor antagonist. ***A***, Left, Fluorescence image of sagittal brain section of ChAT $^{+/IRES\text{-}cre}$ (ChAT-cre) mouse showing labeled CINs expressing ChR2-EYFP overlaid onto corresponding sections from the mouse brain atlas (Franklin and Paxinos, 2007). Scale bar, 400 μm. Right, Fluorescence image of labeled cell bodies and processes of CINs in the NAc shell area. Scale bar, 50 μm. ***B***, Representative current–voltage plot of CIN-oDA. ***C***, Representative CIN-oDA traces with single stimulation (1p), or trains of 4 at 2, 5, or 10 Hz in ACSF (top) and in the presence of the D2 receptor antagonist sulpiride (1 μM, bottom) either in (left) core or in (right) shell area of NAc. Dotted lines represent the baseline and the peak amplitude of CIN-oDA with single stimulation. Blue ticks represent the optogenetic stimulations. Scale bars, 200 nM and 2 s. ***D***, ***E***, Peak amplitudes (***D***) or areas (***E***) normalized by CIN-oDA transients by single pulse (1p) in ACSF plotted as a function of stimulation patterns in dorsal striatum (left), core (middle), and shell (right). $*p < 0.05$, $**p < 0.01$, $***p < 0.001$.

ministration of AAV5 vector with Cre-dependent ChR2-EYFP DA transients were evoked by brief (0.6 ms) 470 nm light pulses around the area showing the expression of EYFP and measured using FSCV. DA transients evoked by optogenetic stimulation of CINs (CIN-oDA) showed the characteristic oxidation and reduction profile of DA (Fig. 1*B*). In the core region, the amplitude of CIN-oDA in response to train stimulation were practically indistinguishable from the DA transient in response to single stimulation (Fig. 1*C*) as previously reported in the dorsal striatum region (Threlfell et al., 2012). Both the peak amplitude (Fig. 1*D*) and the area underneath the curve (Fig. 1*E*) of CIN-oDA in the core and dorsal striatum revealed the insensitivity to stimulation frequency between 2 and 10 Hz ($F \leq 0.83$, $p \geq 0.45$ for the peak and area, $n = 6$ slices/5 mice), except for a slight decrease

in the peak at 5 Hz in dorsal striatum (0.96 ± 0.01 of 1p, $p = 0.001$).

However, in the shell region, the peak amplitude of CIN-oDA evoked by train stimulation at 10 Hz was significantly larger compared with single pulse (33 ± 10% increase, $n = 9$ slices/5 mice, $p = 0.036$ from Tukey's multiple-comparisons test; Fig. 1*C*,*D*). The frequency-dependent summation became more evident when the areas under the curve of CIN-oDA were compared (52 ± 14% increase, $p = 0.02$ with 2 Hz; 36 ± 12%, $p = 0.067$ with 5 Hz; 88 ± 22%, $p = 0.016$ with 10 Hz; $n = 9$ slices/5 mice; Fig. 1*E*). These results suggest that DA transients in the shell show summation compared with other striatal subregions when stimulated with train of pulses at different frequency.

To determine whether the lack of summation of CIN-oDA in the core and dorsal striatum is due to the activation of D2/3 receptors by initial DA release, we performed similar train stimulation experiments in the presence of the DA D2-like receptor antagonist sulpiride (1 μM) and frequency-dependent summation of CIN-oDA was observed in all three regions (Fig. 1*C*,*E*). Sulpiride had no effect on the peak or area of CIN-oDA evoked by single pulses ($p > 0.999$ for peaks and areas from all three regions; Fig. 1*D*,*E*), in agreement with previous studies using electrical stimulation (Trout and Kruk, 1992; Wieczorek and Kruk, 1995). Sulpiride increased the peak amplitude of CIN-oDA evoked by train only in the shell ($F_{1.02,\ 7.13} = 9.47$, $p = 0.017$; Fig. 1*C*,*D*), with no increase in the core and dorsal striatum ($F_{1.72,\ 8.59} = 2.89$, $p = 0.114$ for the core region and $F_{1.98,\ 9.88} = 2.04$, $p = 0.182$ for the dorsal striatum region; Fig. 1*C*,*D*).

For the area of the CIN-oDA transients, sulpiride had effects at most frequencies in all striatal regions (Fig. 1*E*). In the core and dorsal striatum, the area of CIN-oDA with train increased after blocking the D2/3 receptors (core: 105 ± 2% in ACSF vs 168 ± 22% in sulpiride, $p = 0.003$ for 2 Hz and 100 ± 3% in ACSF vs 153 ± 21% in sulpiride, $p = 0.02$ for 5 Hz; dorsal striatum: 116 ± 9% in ACSF vs 205 ± 15% in sulpiride, $p < 0.001$ for 2 Hz and 100 ± 6% in ACSF vs 147 ± 17% in sulpiride, $p = 0.004$ for 5 Hz), but decreased with 10 Hz frequency. In the shell, the increase was more pronounced where the responses to trains were larger after blocking D2/3 receptors (136 ± 12% in ACSF vs 359 ± 69%% in sulpiride, $p = 0.002$ for 5 Hz and 188 ± 22% in ACSF vs 291 ± 84% in sulpiride, $p = 0.006$ for 10 Hz, Bonferroni's multiple-comparisons test). These results suggest that, during the train stimulation, D2/3 receptors are activated by the endogenously released DA and suppress subsequent release of DA, exerting use-dependent inhibition. Furthermore, the data indicate that this D2/3-receptor-mediated inhibition is more evident in the shell region.

D2/3 receptors in CIN and DAN terminals mediate different components of use-dependent inhibition of DA release

To further investigate how DA release is modulated by D2/3 receptors during train stimulation in the shell, we conducted experiments measuring CIN-oDA evoked by paired-pulse stimulations using different intervals (Fig. 2). For shorter intervals, the responses to the second pulse (P2) were assessed offline by subtracting the responses to single pulse from paired-pulse responses (Fig. 2*A*, dotted line). The paired-pulse ratios (PPRs; P2/P1) were plotted as a function of interstimulus interval (ISI) (Fig. 2*B*, black) and showed a marked depression in response to the P2 stimulus at all ISIs. The long-lasting component of P2 depression was reported previously in the nucleus accumbens and dorsal striatum (Cachope et al., 2012; Wang et al., 2014). This phenomenon may be caused by the intrinsic release properties of DAN terminals because DA release evoked by direct optogenetic stimulation of DAN terminals also shows a slow recovery of the P2 depression that takes up to hundreds of seconds (Adrover et al., 2014), which might reflect vesicle depletion (Wang et al., 2014).

The P2 depression of CIN-oDA was even more pronounced with short ISIs (100–500 ms) than longer ISIs. We thus tested whether this was due to a lack of fidelity of ChR2-evoked firing of CINs during the second pulse because ChR2 undergoes inactivation (Lin, 2011) and fails to evoke action potentials reliably at frequencies >25 Hz (Lin et al., 2009). When optogenetic evoked action potentials were recorded in CINs from the NAc shell in cell-attached mode (Fig. 2*C*), the fidelity was near 100% for ISIs of 100 ms or longer (100 ± 0% for 100 ms; 96 ± 4% for 200 ms; 96 ± 4% for 500 ms; $p > 0.05$ for all the ISIs; $n = 9$ cells/4 mice; Fig. 2*C*). With 50 ms, the second pulse evoked an action potential on 88 ± 8% and 11 ± 11% for ISI of 10 ms. Therefore, this result rules out that the marked depression in P2 is due to the lack of fidelity of action potential generation during the second pulse for 100 ms or longer ISIs.

The D2/3 receptor antagonist sulpiride (1 μM) partially relieved the depression of responses to P2, especially with ISIs shorter than 1 s ($PPR_{sulp} - PPR_{ACSF}$: 0.19 ± 0.06, $p = 0.01$ for 200 ms; 0.27 ± 0.06, $p < 0.001$ for 500 ms; Fig. 2*B*). The time course of D2/3-receptor-mediated depression of P2 was assessed by subtracting the PPR curve in ACSF from the curve in sulpiride (Fig. 2*E*), which shows that D2/3 receptor activation by endogenously released DA takes place as early as 100 ms and reaches a maximum by ~500 ms. This onset of D2/3-receptor-mediated inhibition of CIN-oDA is within the range previously reported with electrically evoked DA transients (Phillips et al., 2002).

D2/3 receptor-mediated inhibition of CIN-oDA could be mediated by one or multiple sources of D2 receptors and by D3 receptors known to be more abundant in the shell (Maina and Mathews, 2010). D2 receptors in CINs that inhibit ACh release can subsequently diminish DA release evoked by CINs and D2/3 autoreceptors can also inhibit DA release directly at DAN terminals. In this study, we focus on the contribution of the two pools of D2 receptors to the use-dependent inhibition and generated cell-specific Drd2 knock-out mice with targeted deletion of D2 receptors from CINs (ChAT-cre × $Drd2^{loxP/loxP}$, referred as CINDrd2KO) to isolate its contribution (Fig. 2*D*). Mice lacking D2 receptors in CINs showed less P2 depression of CIN-oDA at shorter ISIs compared with control ChAT-cre animals in ACSF ($PPR_{CINDrd2KO} - PPR_{ChAT\text{-}cre}$: 0.58 ± 0.06 for 100 ms; 0.30 ± 0.06 for 200 ms; 2-way RM ANOVA genotype × PPI interaction $F_{(6,126)} = 13.03$, $p < 0.001$; *post hoc t* test, $p < 0.001$), but not different at ISIs ≥ 500 ms (Fig. 2*B*,*D*). In these knock-out animals, addition of sulpiride had no effect on P2 depression at the 100 ms interval, but D2/3 receptor modulation at ~500 ms was larger than in ChAT-cre controls (Fig. 2*D*,*E*). The onset of D2/3-receptor-mediated inhibition was delayed, suggesting that D2 receptors in CINs are responsible for the early component of the use-dependent inhibition at ~100 ms. This finding also implies that the remaining component of the use-dependent inhibition is not due to D2 receptors in CINs, but rather is likely due to D2/3 autoreceptors in DAN terminals.

To isolate the contribution of D2 autoreceptors, we measured DA transients evoked by optogenetic stimulation of DAN axons (DAN-oDA) using paired-pulse stimulation in the shell region of DAT-cre mice. The transients evoked by DAN axons stimulation had similar amplitudes (253 ± 16 nM for DAN-oDA, $n = 31$

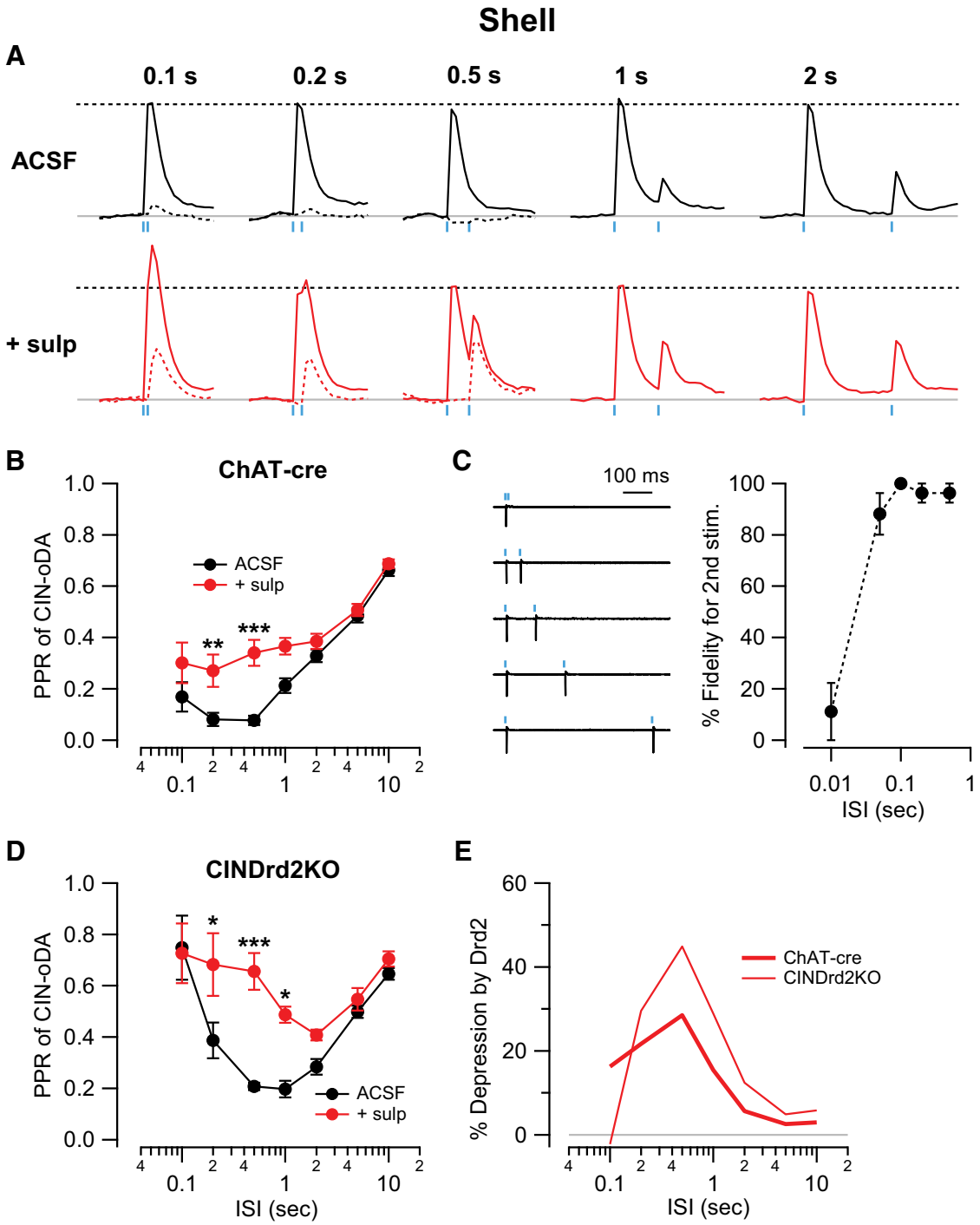

Figure 2. Early phase of the D2-receptor-mediated depression of CIN-oDA in the shell is through D2 receptors in CINs. ***A***, Representative traces of CIN-oDA evoked by paired-pulse stimulations with different ISIs (0.1, 0.2, 0.5, 1, or 2 s) in ACSF (top) and in the presence of sulpiride (1 μM, bottom) in the shell area of ChAT-cre mice. CIN-oDA transients evoked by the second pulse (dotted) were calculated by subtracting the single-pulse CIN-oDA transients for ISIs between 0.1 and 2 s. Blue ticks represent the optogenetic stimulations. ***B***, PPRs (P2/P1) of CIN-oDA measured in the shell area of ChAT-cre mice were plotted as a function of ISI in ACSF (black) or in the presence of sulpiride (red). ***C***, Left, Representative traces of cell-attached patch recordings from a CIN showing action potentials in response to paired optogenetic stimulations (blue ticks) with different ISIs: 0.01, 0.05, 0.1, 0.2, and 0.5 s. Right, Fidelity for second stimulation was calculated as the percentage of successfully evoked action potentials by the second stimulation and plotted as a function of ISI. ***D***, PPR of CIN-oDA measured in the shell area of ChAT-cre × Drd2$^{loxP/loxP}$ (CIND2rdKO) mice plotted as a function of ISI in ACSF (black) or in the presence of sulpiride (red). ***E***, Degree of depression in P2 due to DA D2/3 receptor activation was assessed by subtracting the PPR curves in ACSF from the PPR curve in the presence of sulpiride either from ChAT-cre mice (thick) or from CINDrd2KO mice (thin). *$p < 0.05$, **$p < 0.01$, ***$p < 0.001$.

slices/9 mice; 261 ± 15 nM for CIN-oDA, n = 45/17 mice; unpaired t test $p = 0.71$), but showed slower decay (0.35 ± 0.02 s for DAN-oDA; 0.25 ± 0.01 for CIN-oDA; $p < 0.001$; Fig. 3*A*), possibly reflecting differences in reuptake, as described previously (O'Neill et al., 2017). The PPR curve of DAN-oDA showed the characteristic U-shape, as described previously (Adrover et al., 2014; Fig. 3*B*). The increase in PPRs at shorter ISIs suggests that a supralinear relationship exists between Ca^{2+} concentration and the release probability in DAN terminals in addition to the aforementioned vesicle depletion hypothesis.

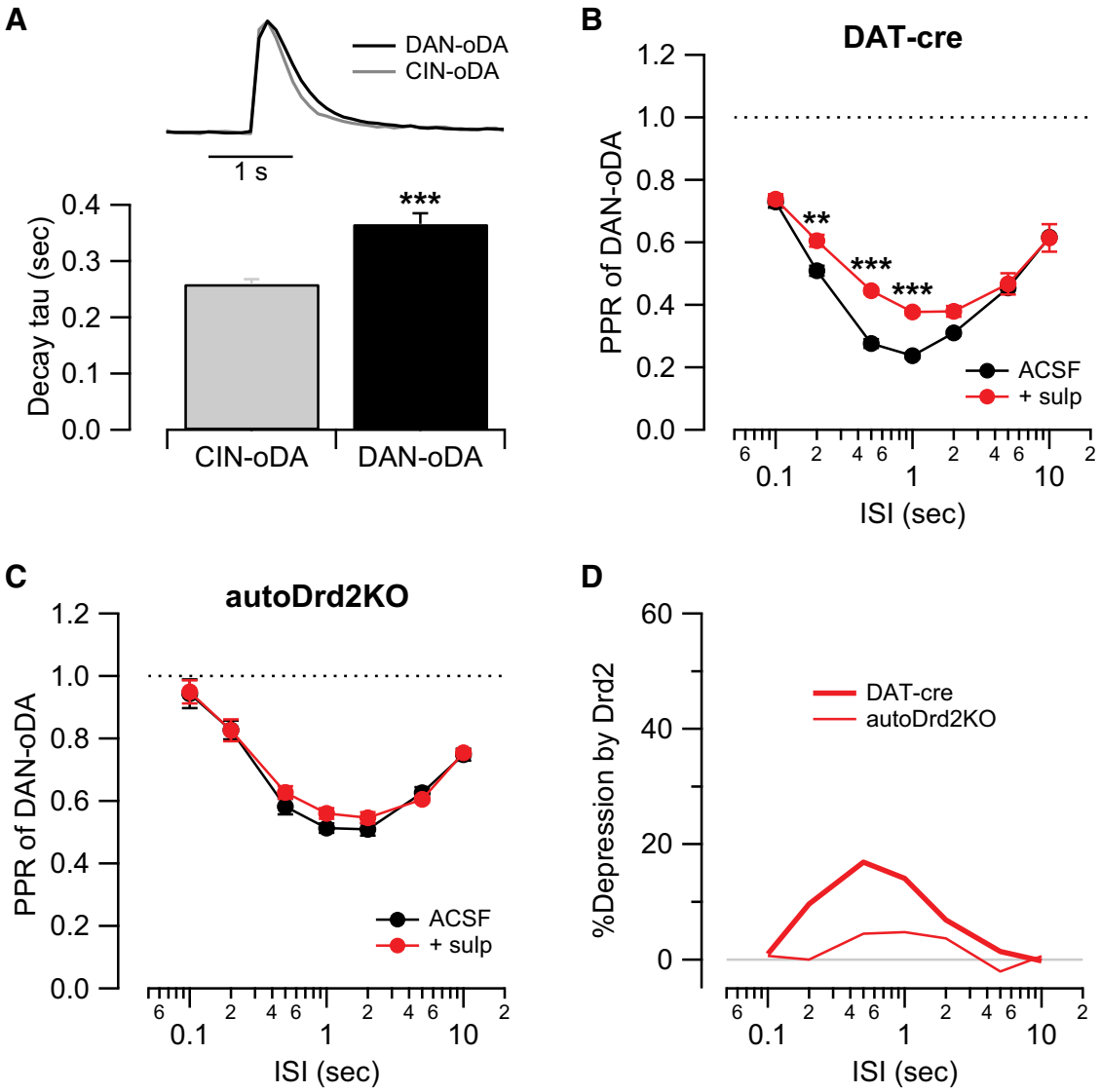

Figure 3. D2 autoreceptors on the DAN terminals are responsible for the late phase of D2-receptor-mediated inhibition of DA release. ***A***, Top, Representative traces of DAN-oDA (black) and CIN-oDA (gray). Bottom, Decay tau's plotted as bar graph (average ± SEM). ***B***, ***C***, PPRs of DAN-oDA measured in the shell area of either DAT-cre (***B***) or DAT-cre × Drd2 $^{loxP/loxP}$ (autoDrd2KO; ***C***) mice plotted as a function of ISI in ACSF (black) or in the presence of sulpiride (1 μM, red) in the shell area. ***D***, Degree of depression in P2 due to DA D2 autoreceptors activation was assessed as described previously and plotted as a function of ISI either from DAT-cre mice (thick line) or from autoDrd2KO (thin line). $^{**}p < 0.01$, $^{***}p < 0.001$.

Application of sulpiride significantly attenuated the depression of P2 for ISIs of 200 ms, 500 ms, and 1 s [$PPR_{sulp} - PPR_{ACSF}$: 0.10 ± 0.03 for 200 ms; 0.17 ± 0.03 for 500 ms; 0.14 ± 0.03 for 1 s; 2-way repeated-measures (RM) ANOVA pharmacology × ISI interaction $F_{(6,168)} = 6.174$, $p < 0.001$; *post hoc t* test $p = 0.003$ for 200 ms and $p < 0.001$ for 500 ms and 1 s; Fig. 3*B*,*D*]. Sulpiride had no effect on ISIs longer than 2 s, indicating that P2 depression at longer intervals is not mediated by D2/3 receptors.

Because DAN-oDA is independent of CIN activity and nAChR activation, this sulpiride-mediated relief in P2 depression is most likely due to D2 and D3 autoreceptors in DAN terminals. In fact, when D2 autoreceptors were deleted selectively in DANs (DAT-cre × Drd2 $^{loxP/loxP}$, referred as autoDrd2KO), most of sulpiride relief of the DAN-oDA was lost (2-way ANOVA no interaction $F_{(6,55)} = 0.85$, $p = 0.54$; no main effect with pharmacology $F_{(1,55)} = 2.59$, $p = 0.11$; Fig. 3*C*,*D*). Furthermore, in autoDrd2KO mice, the PPR curve in ACSF was almost overlapping with the curve in sulpiride. A small fraction of remaining inhibition was observed (Fig. 3*C*,*D*) and is likely mediated by D3 autoreceptors in DAN terminals. Therefore, in the shell, D2 autoreceptors are responsible for most of the use-dependent inhibition of DA release of DAN-oDA.

This D2 autoreceptor-mediated inhibition of P2 is not present at 100 ms and only becomes apparent after 200 ms, with a maximum at ~500 ms (no effect seen for ISIs > 2 s). Therefore, the onset of the D2-autoreceptor-mediated inhibition of DAN-oDA (Fig. 3*D*) is delayed compared with the onset of the D2-receptor-mediated inhibition of P2 in CIN-oDA from control ChAT-cre mice (Fig. 2*E*). In addition, the time course of the autoreceptor-mediated inhibition of DAN-oDA resembles the time course of CIN-oDA from mice lacking the D2 receptor in CINs (CINDrd2KO; Fig. 2*E*). These findings suggest that the early onset (~100 ms) of the use-dependent modulation by D2 receptors is mediated by D2 receptors in CINs and the late component (~500 ms) is mediated by D2 autoreceptors in DAN terminals.

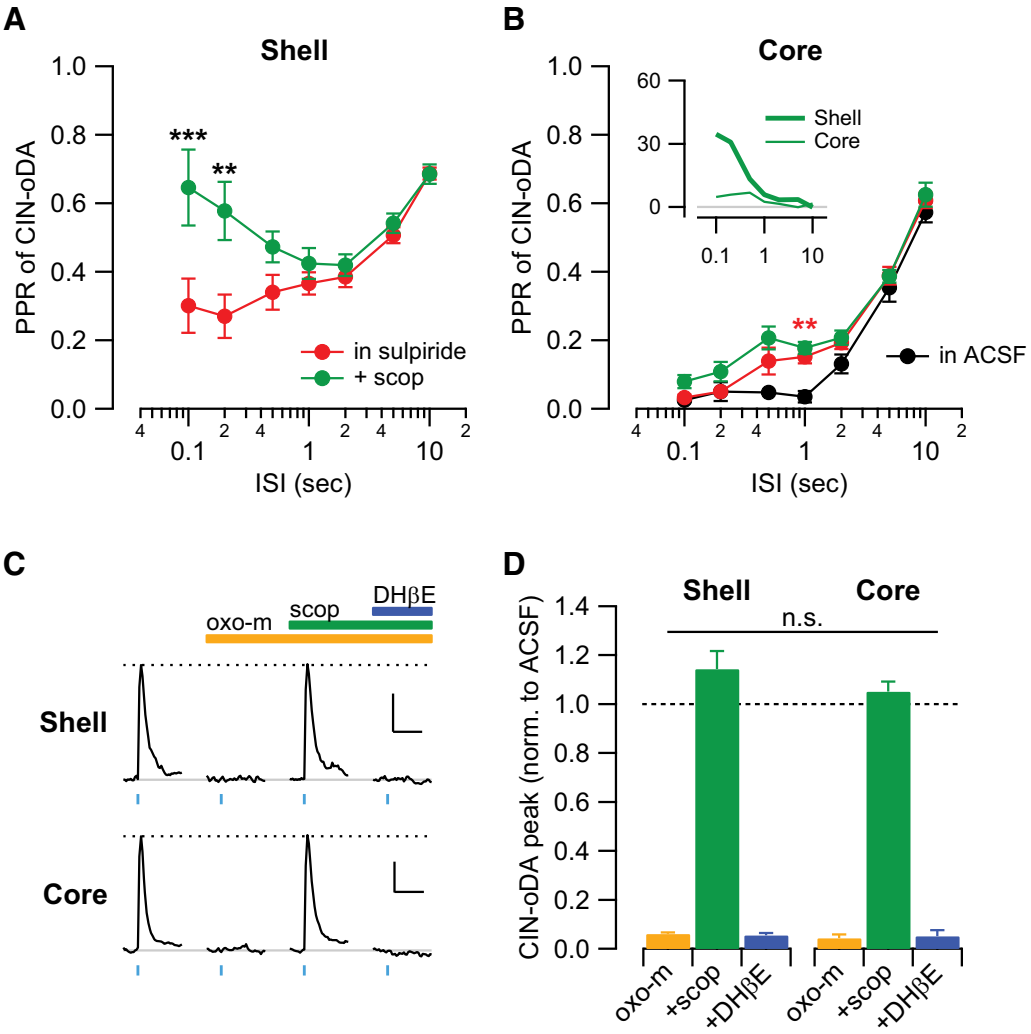

Figure 4. mAChRs also contribute to the use-dependent inhibition of CIN-oDA in the shell but significantly less in the core region. ***A***, ***B***, PPRs of CIN-oDA either in the shell (***A***) or in the core regions (***B***) of ChAT-cre mice plotted as a function of ISI in the presence of sulpiride (red) or after application of the nonspecific mAChR antagonist scopolamine (1 μM, green). Inset, Degree of depression in P2 due to mAChRs activation was assessed as described previously and plotted as a function of ISI either from the shell (thick line) or the core (thin line) regions of ChAT-cre mice. ***C***, Representative traces of CIN-oDA in the shell (top) and the core (bottom) from ChAT-cre mice with sequential application of the nonspecific mAChR agonit oxotremorine (oxo-m; 10 μM), scopolamine, and the β2-containing nAChR antagonist DHβE (1 μM). Dotted lines represent the peak amplitude of CIN-oDA in ACSF. Blue ticks represent the optogenetic stimulations. Scale bars, 200 nM and 2 s. ***D***, Drug effects plotted as bar graph of CIN-oDA peak amplitudes normalized to their baselines in ACSF (average ± SEM) from each region. $^{**}p < 0.01$, $^{***}p < 0.001$.

mAChRs in CINs also contribute to the use-dependent inhibition of DA release

Different subtypes of mAChRs are expressed in the striatum (Weiner et al., 1990; Hersch et al., 1994) and are known to modulate the release of DA. M2/4 mAChRs in CIN terminals depress the electrically evoked DA transients by inhibiting the release of ACh (Threlfell et al., 2010; Shin et al., 2015), M5 in DAN terminals potentiates the release of DA (Shin et al., 2015), and M4 mAChRs in D1 medium spiny neurons depresses the release of DA through endocannabinoid production and activation of CB2Rs (Foster et al., 2016). To examine the contribution of mAChRs to the use-dependent inhibition of CIN-oDA, the PPR curve was obtained before and after administration of the nonselective muscarinic antagonist scopolamine (1 μM). These experiments were performed in the presence of sulpiride to remove the D2/3-receptor-mediated modulation. As shown in Figure 4*A*, scopolamine further relieved the inhibition of P2 responses with shorter ISIs only in the shell ($PPR_{sulp/scop} - PPR_{sulp}$: 0.34 ± 0.08 for 100 ms; 0.31 ± 0.08 for 200 ms; 2-way ANOVA pharmacology × ISI interaction $F_{(6,181)} = 2.95$, $p = 0.009$; *post hoc t* test $p < 0.001$ for 100 ms and $p = 0.002$ for 200 ms). Scopolamine had no effect on the PPR curve in the core region (2-way RM ANOVA no interaction $F_{(6,48)} = 0.63$, $p = 0.70$; no main effect with pharmacology $F_{(1,8)} = 3.77$, $p = 0.09$; Fig. 4*B*). These data suggest that mAChRs also contribute to the use-dependent inhibition of CIN-oDA mainly in the shell region.

One factor that may contribute is the regional difference in mAChR-mediated inhibition either due to low levels of receptor expression and/or lower coupling efficiency. However, the muscarinic agonist oxotremorine (10 μM) similarly abolished CIN-oDA evoked by single pulse in both the shell and core regions (2-way RM ANOVA no interaction $F_{(2,10)} = 0.85$, $p = 0.46$; no main effect with region $F_{(1,5)} = 1.03$, $p = 0.36$; Fig. 4*C*,*D*). Scopolamine (1 μM) fully reversed oxotremorine effects on CIN-oDA and the transients were also completely abolished by the nicotinic receptor antagonist DHβE (1 μM), confirming that CIN-oDA is dependent on nAChR activation (Fig. 4*C*,*D*). Therefore, there is no evidence for regional differences in mAChR-

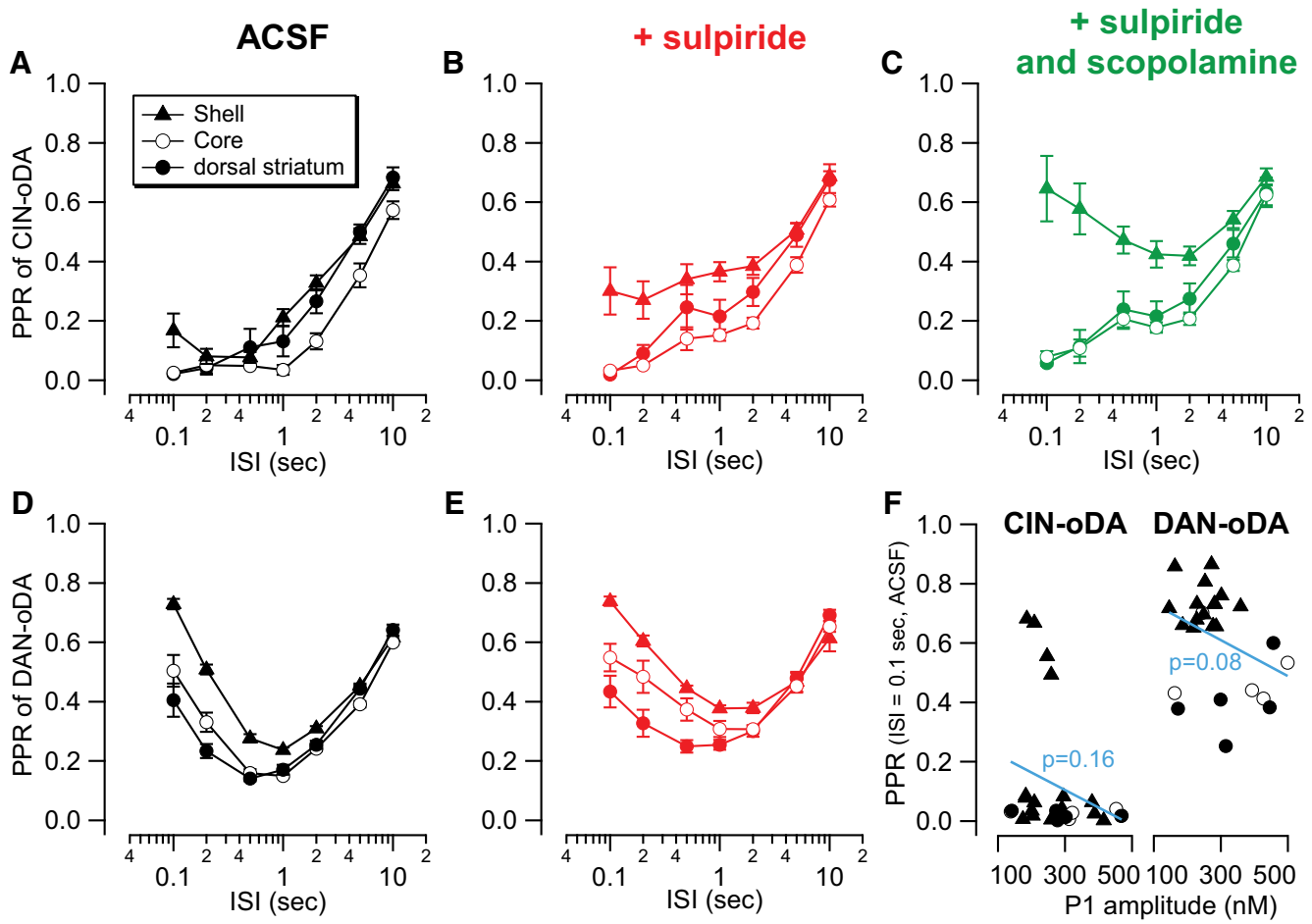

Figure 5. PPR curves of CIN-oDA and DAN-oDA from three different striatal regions for each pharmacological condition. ***A–C***, PPR curves of CIN-oDA from three different striatal regions plotted for comparison in ACSF (***A***), with sulpiride (1 μM; ***B***), and with sulpiride and scopolamine (1 μM; ***C***). ***D***, ***E***, PPR curves of DAN-oDA in ACSF (***D***) and with sulpiride (***E***). ***F***, PPR values of CIN-oDA (left) and DAN-oDA (right) with 0.1 s interval in ACSF plotted as a function of the P1 amplitudes for individual recordings from three different striatal regions. The blue lines represent the linear regression between the PPR values and the P1 amplitudes from all the striatal regions in each group. The *p*-values represent significant difference from zero slope.

mediated inhibition and the lack of relief of the paired-pulse depression by scopolamine in the core region is unlikely due to lower expression or coupling efficiency of mAChRs.

Another possible explanation is that this regional difference is due to a difference in DA release properties of DAN terminals. To address this, we compared the PPR curves and the response to trains of stimulation pulses for DAN-oDA in the different striatal regions. The PPR curves for DAN-oDA showed higher values than CIN-oDA at short intervals for all striatal regions ($p < 0.001$ for ISIs $\leq$ 500 ms in shell; $p < 0.05$ ISIs $\leq$ 2 s in core; $p < 0.001$ for ISIs $\leq$ 200 ms in dorsal striatum; Bonferroni's multiple-comparisons test; Fig. 5*A*,*D*), suggesting that DAN terminals are capable of more release at short intervals than the release seen during CINs evoked DA release. Sulpiride further increased the PPR values for DAN-oDA also in the core for 200–1000 ms ISIs, but not at shorter intervals (Fig. 5*E*), similar to data from shell (Fig. 3*B*). There was no relief of DAN-oDA depression by sulpiride in the dorsal striatum at all ISIs tested. Therefore, small regional differences were seen at the shortest interval where the shell showed the highest values of PPR compared with the core and the dorsal striatum both in ACSF ($PPR_{Shell} - PPR_{Core}$: 0.23 ± 0.03 for 100 ms, *post hoc*) and in sulpiride ($PPR_{Shell} - PPR_{Core}$: 0.19 ± 0.05 for 100 ms, *post hoc t* test $p < 0.001$; 0.12 ± 0.05 for 200 ms, $p = 0.08$; 2-way RM ANOVA region × PPI interaction $F_{(6,108)} = 2.38$, $p = 0.034$; Fig. 5). Because DAN terminals can undergo depletion after the initial release (Wang et al., 2014), PPR values may depend on the P1 amplitude, which may explain the differences between regions and between CIN-oDA and DAN-oDA. However, the P1 amplitudes were not significantly different between regions and between stimulations (CIN-oDA: 292.4 ± 52.0 nM for dorsal striatum, 338.7 ± 59.8 nM for core, 257.2 ± 18.7 nM for shell; DAN-oDA: 337.9 ± 52.5 nM for dorsal striatum, 345.2 ± 61.8 nM for core, 248.6 ± 14.4 nM for shell; $F_{(5,46)} = 1.846$, $p = 0.1225$; one-way ANOVA). Furthermore, there was no correlation between P1 and PPR values from all the recordings with ISI = 0.1 s when the degree of depletion may be highest (CIN-oDA: $F_{(1,25)} = 2.028$, $p = 0.17$, $r^2 = 0.075$; DAN-oDA: $F_{(1,23)} = 3.311$, $p = 0.08$, $r^2 = 0.126$; linear regression; Fig. 5*F*). Differences in PPR between regions and between stimulations cannot be explained by depletion.

The response to trains of pulses also showed significant summation in the peak of DAN-oDA in all striatum regions (dorsal striatum: 30.3 ± 6.4%, $p = 0.02$ for 10 Hz, $n = 6$ slices/2 mice; core: 31.0 ± 8.1%, $p = 0.04$ for 5 Hz and 95.2 ± 6.7%, $p < 0.001$ for 10 Hz, $n = 6$ slices/3 mice; shell: 48.4 ± 10.9%, $p = 0.009$ for 5 Hz and 129.9 ± 9.6% increase for 10 Hz, $p < 0.001$, $n = 9$ slices/3 mice; all from Tukey's multiple-comparisons test; Fig. 6*A*,*B*). This summation in the response to trains of pulse was more apparent when scored with the area of DAN-oDA (dorsal striatum: 16.4 ± 3.7%, $p = 0.03$ for 2 Hz, 35.7 ± 7.6%, $p = 0.02$

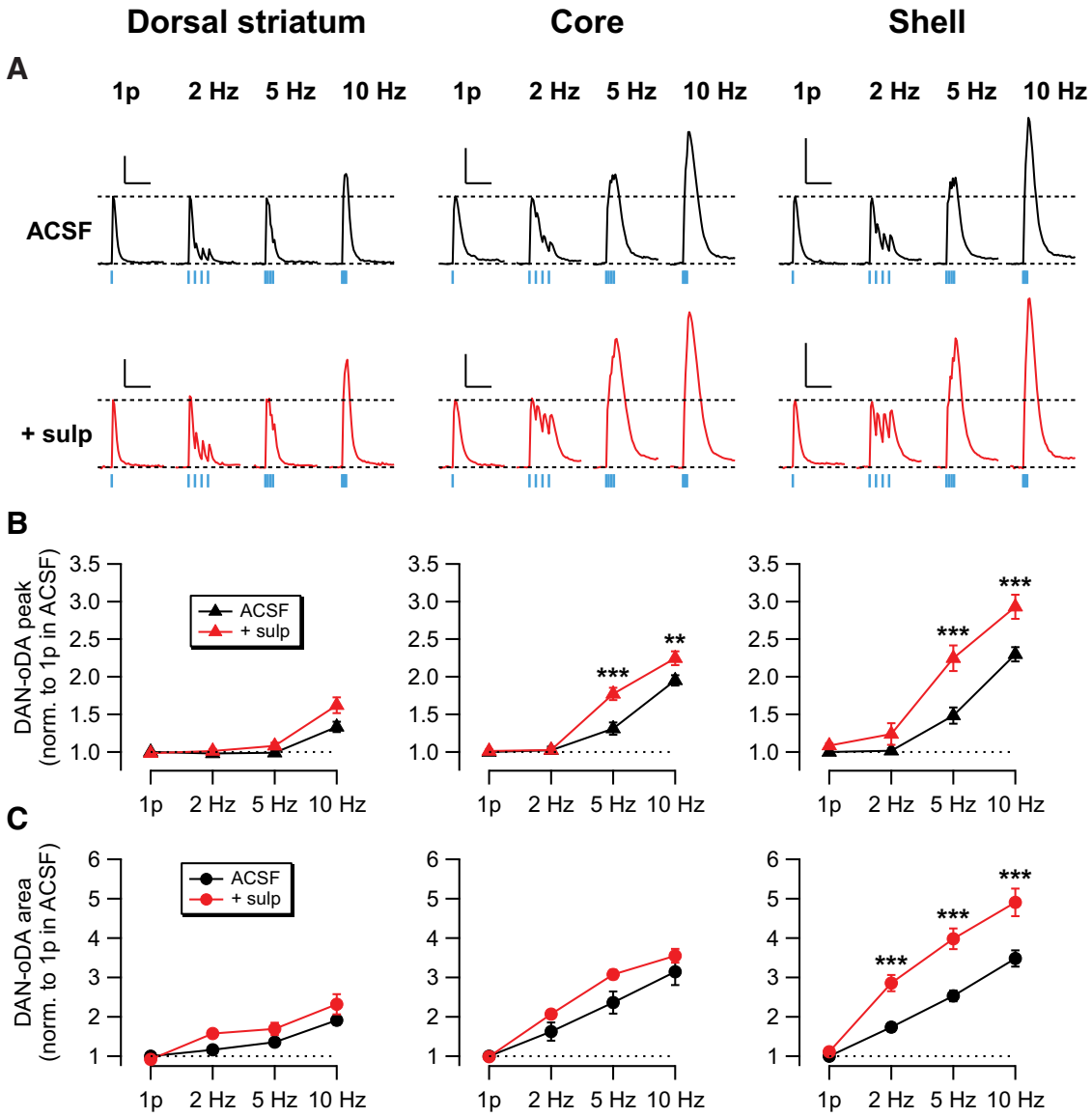

Figure 6. DA release evoked by optogenetic stimulation of DAN axons shows frequency-dependent summation in all striatal region and a further increase in the presence of D2 receptor antagonist. ***A***, Representative DAN-oDA traces with single stimulation (1p) and trains of 4 pulses at 2, 5, and 10 Hz in dorsal striatum, NAc core, and shell in ACSF (top) and in the presence of the D2 receptor antagonist sulpiride (1 μM, bottom). Dotted lines represent the baseline and the peak amplitude of DAN-oDA with single stimulation. Blue ticks represent the timing of optogenetic stimulations. Scale bars, 200 nM and 2 s. ***B***, ***C***, Peak amplitudes (***B***) or areas normalized by DAN-oDA transients by single pulse (1p; ***C***) in ACSF plotted as a function of stimulation patterns in dorsal striatum (left), core (middle), and shell (right). $^{**}p < 0.01$, $^{***}p < 0.001$.

for 5 Hz, 91.4 ± 11.1%, $p = 0.002$ for 10 Hz; core: 136.1 ± 28.4%, $p = 0.018$ for 5 Hz and 214.4 ± 33.5%, $p = 0.005$ for 10 Hz; shell: 73.8 ± 10.8% for 2 Hz, 153.2 ± 13.6% for 5 Hz, and 248.4 ± 20.1% increase, $p < 0.001$ for all frequencies; Fig. 6*A*,*C*). These results suggest that terminals from all regions are capable of more release for subsequent stimulation than seen during CIN-evoked release. At the same time, these experiments revealed small regional difference in the response to train of pulses in DAN-oDA, where summation is highest in the shell, followed by the core, and the smallest degree of summation was observed in the dorsal striatum. Important for the scope of this study, sulpiride further enhanced summation in the peak at 5 Hz and 10 Hz in the core and shell region (core: 131 ± 8% in ACSF vs 177 ± 8% in sulpiride, $p < 0.001$ for 5 Hz and 195 ± 7% in ACSF vs 225 ± 9% in sulpiride, $p = 0.006$ for 10 Hz; shell: 145 ± 11% in ACSF vs 225 ± 17% in sulpiride, $p < 0.001$ for 5 Hz and 230 ± 10% in ACSF vs 293 ± 16% in sulpiride, $p < 0.001$ for 10 Hz; Bonferroni's multiple-comparisons test; Fig. 6*B*), but only in the shell regions when scored with the area (174 ± 11% in ACSF vs 285 ± 21% in sulpiride for 2 Hz, 253 ± 14% in ACSF vs 398 ± 26% in sulpiride for 5 Hz, and 348 ± 21% in ACSF vs 490 ± 35% in sulpiride for 10 Hz, $p < 0.001$ for all frequencies; Bonferroni's multiple-comparisons test; Fig. 6*C*). Together, these data indicate that DA release evoked by direct activation of DAN axons is capable of summation in all striatal regions and blockade of D2/3 receptors further enhances summation in the core and shell regions, suggesting engagement of D2 autoreceptor inhibition of DA release in these regions. These experiments also show small regional differences in DA release properties evoked directly by stimulation of DAN axons. Although these small differences are likely to contribute to some extent to the difference seen in CIN-oDA, they cannot fully account for the regional difference in CIN-oDA summation. Therefore, we speculated that other mechanisms override the summation of DA signals and cover up the use-

dependent mAChR- and D2-receptor-mediated inhibition of DA release in the core region.

Clearance of ACh affects release of DA

Endogenously released ACh is cleared mostly by enzymatic degradation by acetylcholinesterase (Quinn, 1987). Histochemical assays report regional differences in the level of acetylcholinesterase activity in the striatum (Záborszky et al., 1985; Voorn et al., 1994; Franklin and Paxinos, 2007). The acetylcholinesterase activity in the core region is lower compared with the shell, suggesting that the clearance of ACh is slower and ACh lasts longer in the core region. It is also known that, once nAChRs are activated, they undergo desensitization when ACh is present continuously (Giniatullin et al., 2005). Therefore, we hypothesized that ACh released from the first pulse desensitizes nAChRs, causing the massive depression of subsequent pulses delivered at short intervals in the core region. nAChR desensitization might mask the use-dependent mAChR- and D2-receptor-mediated modulation in this region. Furthermore, due to the higher level of acetylcholinesterase, released ACh would be cleared more quickly from the shell than the core region, which may account for faster recovery from nAChR desensitization in the shell region and for less paired-pulse depression of CIN-oDA. If this hypothesis is correct, then we can predict that prolonging the increase of ACh in the shell region will enhance nAChR desensitization, resulting in more pronounced paired-pulse depression as in the core region.

To test this hypothesis, we applied the acetylcholinesterase inhibitor ambenonium and obtained the PPR curve in the presence of sulpiride and scopolamine from the shell and core regions (Fig. 7). In the shell region, ambenonium (50 nM) increased the amplitude of CIN-oDA in response to single pulse stimulation (21.4 ± 7.14% increase from the baseline, $n = 8$ slices/5 mice), indicating that ACh clearance can modulate the amplitude of CIN-oDA. This finding is in agreement with data described previously (Zhang et al., 2004) and it is likely caused by larger increase in the extracellular concentration of ACh upon release and more nAChR activation. However, ambenonium decreased the PPR values in the shell region significantly (in sulpiride and scopolamine vs after ambenonium: 0.65 ± 0.12 vs 0.02 ± 0.00 for 100 ms, $p < 0.001$; 0.59 ± 0.09 vs 0.03 ± 0.01 for 200 ms, $p < 0.001$; 0.48 ± 0.05 vs 0.05 ± 0.02 for 500 ms, $p < 0.001$; 0.42 ± 0.04 vs 0.08 ± 0.05 for 1 s, $p = 0.001$; from Bonferroni's multiple-comparisons test; Fig. 7*A*) and to a lesser extent in the core region (in sulpiride and scopolamine vs after ambenonium: 0.25 ± 0.04 vs 0.08 ± 0.04 for 500 ms, $p = 0.03$; 0.21 ± 0.03 vs 0.01 ± 0.01 for 1 s, $p = 0.008$; 0.25 ± 0.03 vs 0.04 ± 0.01 for 2 s, $p = 0.006$; 0.41 ± 0.02 vs 0.22 ± 0.07 for 5 s, $p = 0.01$; 0.64 ± 0.03 vs 0.46 ± 0.11 for 10 s, $p = 0.02$; from Bonferroni's multiple-comparisons test; Fig. 7*B*). In the presence of ambenonium, the PPR curves from the two regions look very similar. Furthermore, the large summation of CIN-oDA seen only in the shell in response to train stimulation was completely abolished by this concentration of ambenonium (in sulpiride and scopolamine vs after ambenonium: 163 ± 12% of CIN-oDA peak to single stimulation vs 105 ± 4% for 5 Hz, $p < 0.001$; 250 ± 20% vs 99 ± 4% for 10 Hz, $p < 0.001$; from Bonferroni's multiple-comparisons test; Fig. 7*C–F*). In summary, the data provide evidence that the activity level of acetylcholinesterase can determine the degrees of summation of the DA signals evoked by CIN and the frequency-dependent modulation of DA release, which are different in the NAc shell compared with the core. Therefore, in agreement with the previous hypothesis by Threlfell et al. (2012), these findings suggest that nAChR desensitization plays an important role in shaping the use-dependent depression of DA signals in the core and dorsal striatum regions, which is less prominent in the shell region, where frequency-dependent summation of DA signals evoked by CIN is larger and signals are more susceptible to use-dependent modulation by mAChR and D2 receptors and autoreceptors.

Discussion

This study characterized the use-dependent inhibition of DA transients evoked by optogenetic stimulation of CIN. The NAc shell shows unique properties that contribute to distinctive modulation of DA transmission not observed in the NAc core and dorsal striatum: frequency-dependent summation in response to train stimulation; depression of subsequent release by D2 receptors and mAChRs; and higher sensitivity to acetylcholinesterase blockade, suggestive of faster degradation of ACh in the shell.

CIN-oDA transients result from a disynaptic mechanism that involves ACh release from CINs, activation of nAChRs in DAN axons, and DA release from DAN terminals (Fig. 8*A*). Here, we show that CIN-oDA in the core region has a frequency insensitivity similar to the dorsal striatum (Threlfell et al., 2012), whereas CIN-oDA in the shell shows modest summation by train stimulation at 10 Hz (Fig. 1). Indeed, the PPR of CIN-oDA at 100 ms interval was significantly higher in the shell region than core and dorsal striatum, where the response to the second pulse was completely depressed (Fig. 5). In the presence of a D2/3 receptor antagonist, CIN-oDA showed greater frequency-dependent summation in the shell region (Fig. 1), but only minor changes in the core and dorsal striatum regions. Similarly, D2/3 receptor antagonism increases the PPRs at shorter intervals, which were further increased by addition of a mAChR antagonist in the shell. Therefore, these results indicate that D2 receptors and mAChRs in the shell contribute to the use-dependent inhibition of CIN-oDA, whereas in the core and dorsal striatum, these receptors contribute far less.

This regional difference in the summation by train stimulation may be explained by the release properties of DA and/or ACh. DA transients evoked by direct stimulation of DAN axons showed small regional difference in the PPR curves (Fig. 5) and both core and shell showed some degree of summation of DAN-oDA signals with train stimulation at 5 and 10 Hz (Fig. 6). The diversity of DANs across the VTA-SNc area with regard to the genetic and electrophysiological properties could underlie the regional differences in release properties seen at the terminals. Therefore, whereas these regional differences in DAN-oDA are small and cannot fully account for the differences, they can contribute to the regional differences seen in CIN-oDA.

A recent study evaluated ACh release in the dorsal striatum using G-protein-activated inwardly rectifying potassium channels overexpressed in medium spiny neurons (Mamaligas and Ford, 2016), where the P2 response was depressed by half at 100 ms ISI. Therefore, it is unlikely that the depression of ACh release entirely accounts for the use-dependent depression of CIN-oDA seen in this region.

As for the regional difference in modulation of CIN-oDA by D2 or mACh receptors, one possibility is that the expression and/or efficacy of these receptors is low in the core and dorsal striatum. However, the D2 receptor agonist quinpirole suppresses CIN-oDA in dorsal striatum (Threlfell et al., 2012) and so does the mAChR agonist oxotremorine in dorsal striatum (Threlfell et al., 2012) and in the core (Fig. 4), indicating that CIN-oDA in core and dorsal striatum can be modulated by these receptors. Indeed, D2/3 receptor antagonism relieves the depression of P2 at 1 s ISI, but not at shorter ISIs (Figs. 4, 5), and also

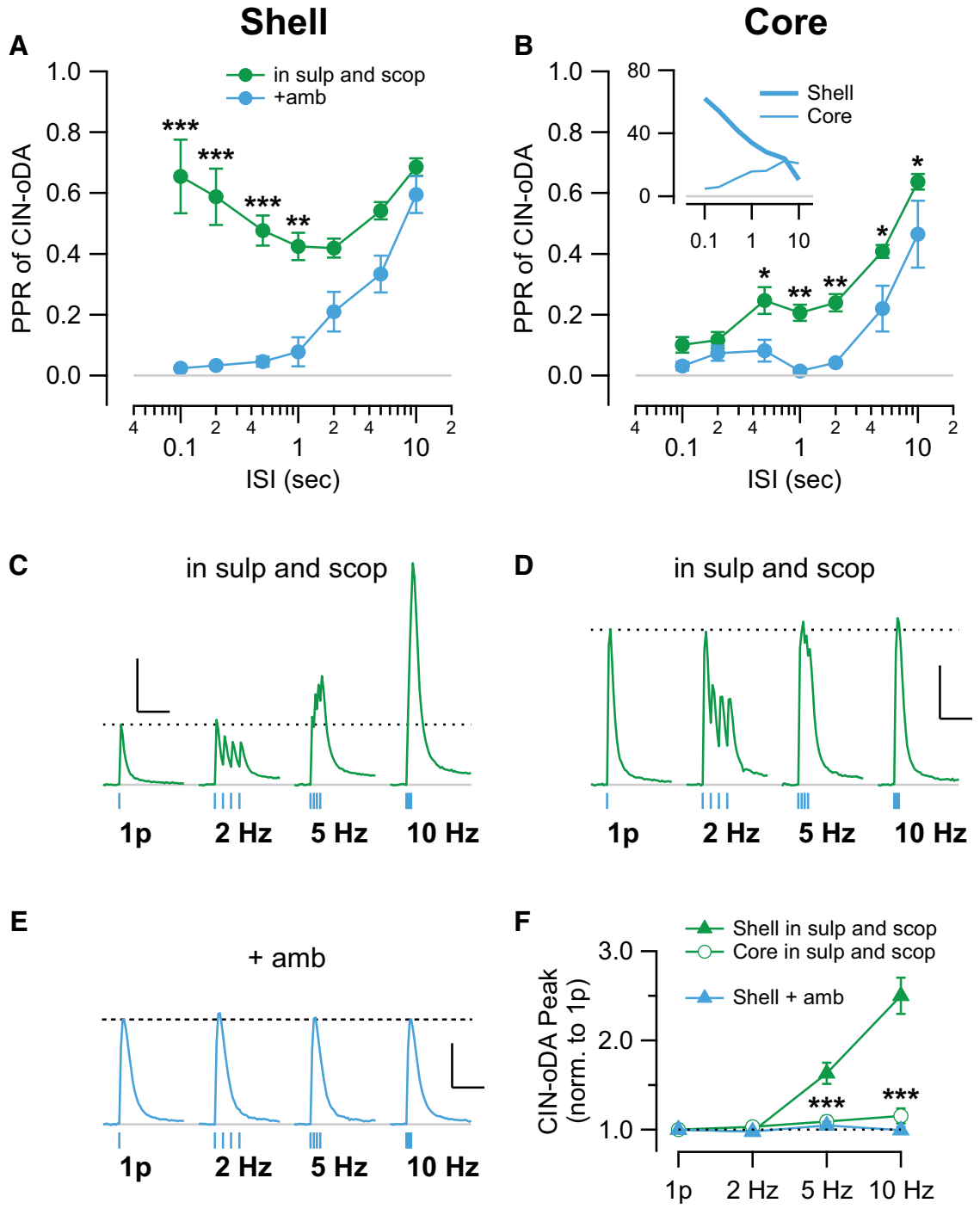

Figure 7. Clearance of ACh by acetylcholinesterase shapes the time course of the use-dependent inhibition of CIN-oDA. ***A***, ***B***, PPRs of CIN-oDA either in the shell (***A***) or in the core regions (***B***) of ChAT-cre mice plotted as a function of ISI in the presence of sulpiride and scopolamine (green) or after application of the acetylcholinesterase blocker ambenonium (50 nM; blue). Inset, Degree of depression in P2 due to blocking acetylcholinesterase was assessed as described previously and plotted as a function of ISI either from the shell (thick line) or the core (thin line) regions of ChAT-cre mice. ***C–E***, Representative CIN-oDA traces with single stimulation (1p) or trains of 4 at 2, 5, or 10 Hz in the presence of sulpiride and scopolamine (left) in the shell (***C***), core (***D***), and in the shell after further application of ambenonium (blue; ***E***). Dotted lines represent the baseline and the peak amplitude of CIN-oDA with single stimulation. Blue ticks represent the optogenetic stimulations. Scale bars, 200 nM and 2 s. ***F***, Peak amplitudes normalized by CIN-oDA transients by single pulse (1p) plotted as a function of stimulation patterns. $^{*}p < 0.05$, $^{**}p < 0.01$, $^{***}p < 0.001$.

relieves CIN-oDA evoked by train stimulation at 2 and 5 Hz, but not at 10 Hz (Fig. 1*C*,*E*), in the core and dorsal striatum. Therefore, it is apparent that there is a mechanism suppressing DA release in response to subsequent stimulations after initial stimulation, which lasts up to 500 ms and masks D2/3 receptor- or mAChR-mediated depression in the core and dorsal striatum.

β2-containing nAChRs in DAN axons are responsible for triggering DA release evoked by synchronous activation of CINs (Cachope et al., 2012; Threlfell et al., 2012), which are prone to desensitization during sustained increases in extracellular ACh or in response to prolonged application of agonists (Giniatullin et al., 2005). nAChR desensitization was proposed as one of the

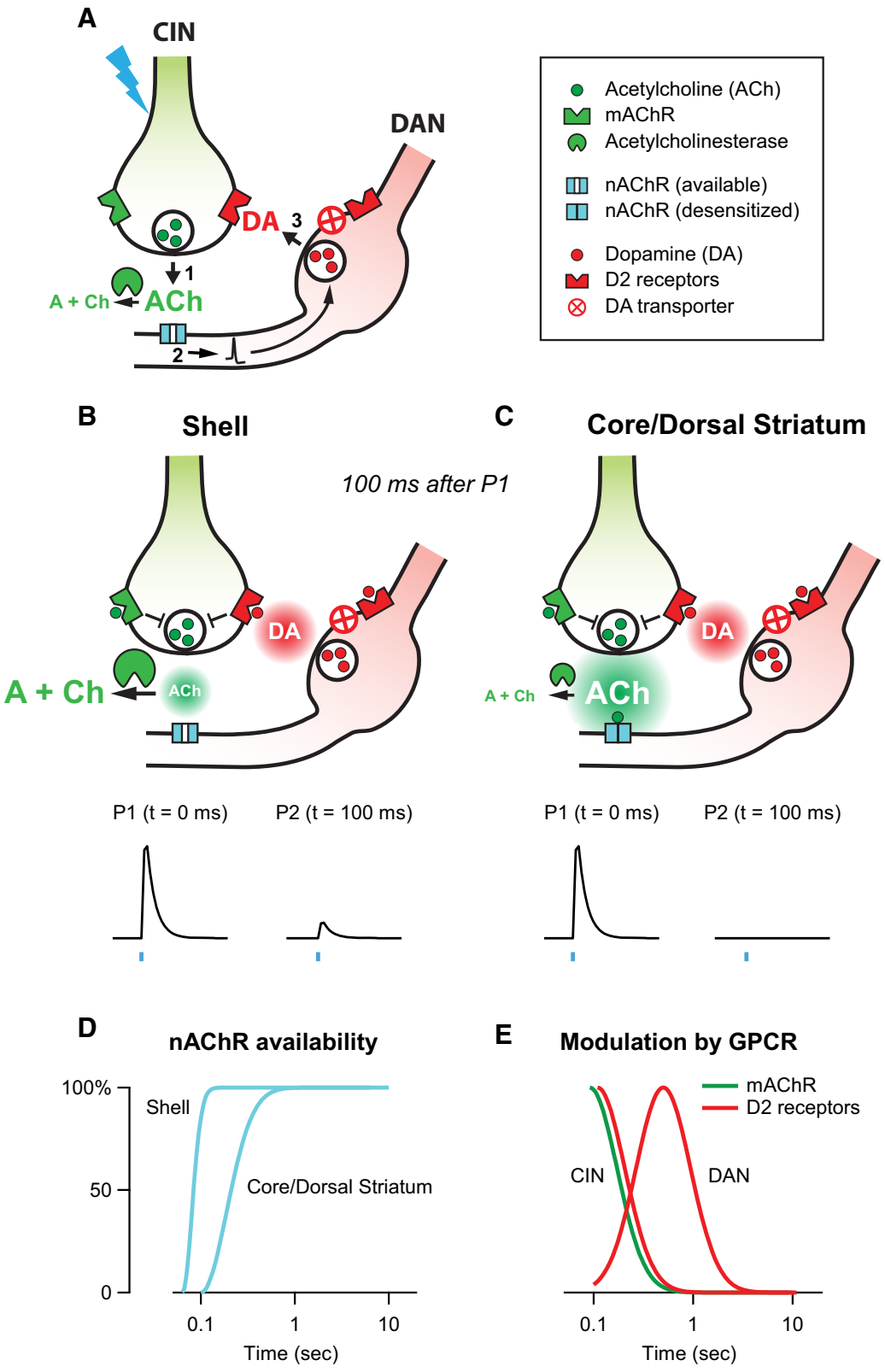

Figure 8. Model of use-dependent inhibition of CIN-evoked DA release by D2 receptors and ACh receptors. ***A***, Diagram showing a disynaptic mechanism of CIN-evoked DA release through: (1) ACh release from CIN terminal, (2) nAChR activation, and (3) DA release from DAN terminal. ***B***, ***C***, Top, Diagrams showing different states 100 ms after the initial stimulation of CIN (P1) in either the shell (***C***) or the core/dorsal striatum (***D***). Different levels of acetylcholinesterase activity produce different rate of ACh clearance in two regions. The higher level of ACh in core/dorsal striatum causes desensitization of nAChRs, resulting in no subsequent DA release by P2 (at 100 ms) independent of ACh release. Bottom, DA transients reflecting DA release at P1 and P2 in the corresponding striatal subregions. ***D***, ***E***, Proposed time courses of nAChR availability (blue; ***D***) after the initial stimulation (P1) in the shell or core/dorsal striatum regions and modulation of DA release by DA Drd2 (red; ***E***) and mAChR (green; ***E***) in CINs and DAN terminals (drawn in arbitrary scale).

mechanisms responsible for the lack of summation in CIN-oDA in dorsal striatum (Threlfell et al., 2012). ACh released from CINs is cleared mainly by acetylcholinesterase and the time course of ACh clearance depends on acetylcholinesterase activity. Therefore, we hypothesized that the activity of acetylcholinesterase could affect the degree of nAChR desensitization upon ACh release, with higher activity leading to lower desensitization and vice versa (Fig. 8*B*,*C*). Indeed, higher acetylcholinesterase activity in the shell region has been reported in different species (Záborszky et al., 1985; Voorn et al., 1994; Franklin and Paxinos, 2007). In this study, we found that impairing ACh clearance with a low dose of the acetylcholinesterase inhibitor ambenonium dramatically depressed subsequent CIN-oDA more in the shell than core region without depressing the P1 response. After the application of the inhibitor, both the PPR and the response to trains from the shell region resembled those from the core and dorsal striatum (Fig. 7). These results suggest that full recovery from nAChR desensitization takes up to 500 ms in the core and dorsal striatum regions, but much less time in the shell region (Fig. 8*D*). Further, these findings provide evidence that acetylcholinesterase expression and activity levels are critical factors determining the extent of nAChR desensitization and shaping the use-dependent inhibition of CIN-oDA across striatal regions. Recently, Salinas et al. (2016) reported that striosome and matrix in the striatum show different dopamine dynamics and cocaine sensitivity using single electrical stimulations. Because these subcompartments are known to have differential expression of several proteins including acetylcholinesterase, it will be interesting to see whether these subcompartments also show different use-dependent modulation similar to our findings.

Our study provides evidence that D2 receptors expressed in CINs and DAN terminals both contribute to the depression of CIN-oDA as early as 100 ms and peak at 500 ms before disappearing at 2 s (Fig. 2*B*,*E*). The early onset of the depression (100 ms) was absent in mice lacking D2 receptors in CIN (CINDrd2KO), suggesting that this early component of the depression is due to D2 receptors on CIN terminals (Fig. 2*D*,*E*). The late component of the depression of CIN-oDA (500 ms) persisted in CINDrd2KO mice and we hypothesized that it is mediated by D2 receptors in DAN terminals (D2 autoreceptors). The time course of the D2-receptor-mediated depression of DAN-oDA developed later (not seen at 100 ms) and reached maximum at 500 ms (Fig. 3*B*,*D*), similarly to CIN-Drd2KO. Mice lacking D2 autoreceptors on DANs confirmed the hypothesis and showed dramatically reduced depression of DAN-oDA with similar late onset.

It is worth noting that the D2-receptor-mediated depression of CIN-oDA observed at the earliest time point measured (100 ms) is in agreement with previous reports of D2-receptor-mediated responses in DANs and CINs (Beckstead et al., 2004; Gantz et al., 2013; Chuhma et al., 2014). This D2-receptor-mediated depression of CIN-oDA develops faster than the depression mediated by D2 autoreceptors on DAN terminals (Fig. 8*E*), suggesting that D2 receptors in CINs are in close proximity to DA release sites and act as postsynaptic receptors to synaptically released DA. Conversely, the slow onset of D2 autoreceptors could reflect physical distance between the release site and the location of D2 autoreceptors. It is also possible that the activity of the DA transporter, which is widely expressed on DAN axons (Zhang et al., 2015), limits the DA concentration around D2 autoreceptors (Fig. 8*A*). Interestingly, mAChRs, which we speculate act as autoreceptors in CINs, showed a fast onset of CIN-oDA depression in the shell that resemble the depression by D2 receptors in CINs (Fig. 8*E*).

In this study, all forms of G_i-coupled receptor modulation of DA release evaluated produced effects on P2 only when delivered within 2 s from P1, indicating that mechanisms other than G-protein-coupled receptor modulation are responsible for the long-lasting P2 depression. Vesicle depletion, replenishment, and vesicle loading are other processes likely to contribute to the slow recovery of P2 and dominate over G-protein modulation of release at longer intervals (Wang et al., 2014).

Mouse lines with cell-specific deletion of D2 receptors have proven useful for studying the contribution of D2 receptors in different cell types. However, findings show that these genetic modifications can also cause long-term changes to the intrinsic properties of DA release (Bello et al., 2011). In the presence of sulpiride, the PPR curves from ChAT-cre and CINDrd2KO are different at ISIs from 100 to 500 ms and overlapping for longer ISIs (Fig. 2*B*,*D*). There was less P2 depression in CINDrd2KO at short ISIs, suggesting that the probability of release of ACh and/or DA is changed after genetic deletion of D2 receptors from CINs. These findings are not entirely surprising considering the well established role of G_i-coupled receptors in long-term plasticity at striatal synapses (Atwood et al., 2014).

In conclusion, this study shows that, although nAChR desensitization is the dominant mechanism in the core and dorsal striatum regions, the frequency insensitivity in the shell region is mainly achieved through the use-dependent activation of D2 receptors (both auto and hetero) and mAChRs. This result also implies that alterations in D2 receptor availability in the shell could have an impact on use-dependent modulation of DA transmission in the shell. Our findings showing distinctive modulation by endogenous DA and ACh *in vitro* could account for the unique features of *in vivo* DA signals in the shell and have far-reaching implications for the functional role of NAc shell region in reward-motivated learning.

References

Adrover MF, Shin JH, Alvarez VA (2014) Glutamate and dopamine transmission from midbrain dopamine neurons share similar release properties but are differentially affected by cocaine. J Neurosci 34:3183–3192. CrossRef Medline

Alcantara AA, Chen V, Herring BE, Mendenhall JM, Berlanga ML (2003) Localization of dopamine D2 receptors on cholinergic interneurons of the dorsal striatum and nucleus accumbens of the rat. Brain Res 986:22–29. CrossRef Medline

Aragona BJ, Cleaveland NA, Stuber GD, Day JJ, Carelli RM, Wightman RM (2008) Preferential enhancement of dopamine transmission within the nucleus accumbens shell by cocaine is attributable to a direct increase in phasic dopamine release events. J Neurosci 28:8821–8831. CrossRef Medline

Aragona BJ, Day JJ, Roitman MF, Cleaveland NA, Wightman RM, Carelli RM (2009) Regional specificity in the real-time development of phasic dopamine transmission patterns during acquisition of a cue-cocaine association in rats. Eur J Neurosci 30:1889–1899. CrossRef Medline

Atwood BK, Lovinger DM, Mathur BN (2014) Presynaptic long-term depression mediated by Gi/o-coupled receptors. Trends Neurosci 37:663–673. CrossRef Medline

Beckstead MJ, Grandy DK, Wickman K, Williams JT (2004) Vesicular dopamine release elicits an inhibitory postsynaptic current in midbrain dopamine neurons. Neuron 42:939–946. CrossRef Medline

Bello EP, Mateo Y, Gelman DM, Noaín D, Shin JH, Low MJ, Alvarez VA, Lovinger DM, Rubinstein M (2011) Cocaine supersensitivity and enhanced motivation for reward in mice lacking dopamine D2 autoreceptors. Nat Neurosci 14:1033–1038. CrossRef Medline

Bossert JM, Poles GC, Wihbey KA, Koya E, Shaham Y (2007) Differential effects of blockade of dopamine D1-family receptors in nucleus accumbens core or shell on reinstatement of heroin seeking induced by contextual and discrete cues. J Neurosci 27:12655–12663. CrossRef Medline

Britt JP, Benaliouad F, McDevitt RA, Stuber GD, Wise RA, Bonci A (2012)

Synaptic and behavioral profile of multiple glutamatergic inputs to the nucleus accumbens. Neuron 76:790–803. CrossRef Medline

Cachope R, Mateo Y, Mathur BN, Irving J, Wang HL, Morales M, Lovinger DM, Cheer JF (2012) Selective activation of cholinergic interneurons enhances accumbal phasic dopamine release: setting the tone for reward processing. Cell Rep 2:33–41. CrossRef Medline

Chuhma N, Mingote S, Moore H, Rayport S (2014) Dopamine neurons control striatal cholinergic neurons via regionally heterogeneous dopamine and glutamate signaling. Neuron 81:901–912. CrossRef Medline

Crombag HS, Bossert JM, Koya E, Shaham Y (2008) Review. Context-induced relapse to drug seeking: a review. Philos Trans R Soc Lond B Biol Sci 363:3233–3243. CrossRef Medline

Di Chiara G, Bassareo V (2007) Reward system and addiction: what dopamine does and doesn't do. Curr Opin Pharmacol 7:69–76. CrossRef Medline

Dreyer JK, Vander Weele CM, Lovic V, Aragona BJ (2016) Functionally distinct dopamine signals in nucleus accumbens core and shell in the freely moving rat. J Neurosci 36:98–112. CrossRef Medline

Everitt BJ, Robbins TW (2005) Neural systems of reinforcement for drug addiction: from actions to habits to compulsion. Nat Neurosci 8:1481–1489. CrossRef Medline

Foster DJ, Wilson JM, Remke DH, Mahmood MS, Uddin MJ, Wess J, Patel S, Marnett LJ, Niswender CM, Jones CK, Xiang Z, Lindsley CW, Rook JM, Conn PJ (2016) Antipsychotic-like effects of M4 positive allosteric modulators are mediated by CB2 receptor-dependent inhibition of dopamine release. Neuron 91:1244–1252. CrossRef Medline

Franklin KBJ, Paxinos G (2007) The mouse brain in stereotaxic coordinates, Ed 3. Amsterdam: Elsevier.

Gantz SC, Bunzow JR, Williams JT (2013) Spontaneous inhibitory synaptic currents mediated by a G protein-coupled receptor. Neuron 78:807–812. CrossRef Medline

Giniatullin R, Nistri A, Yakel JL (2005) Desensitization of nicotinic ACh receptors: shaping cholinergic signaling. Trends Neurosci 28:371–378. CrossRef Medline

Groenewegen HJ, Berendse HW, Haber SN (1993) Organization of the output of the ventral striatopallidal system in the rat: ventral pallidal efferents. Neuroscience 57:113–142. CrossRef Medline

Hersch SM, Gutekunst CA, Rees HD, Heilman CJ, Levey AI (1994) Distribution of m1–m4 muscarinic receptor proteins in the rat striatum: light and electron microscopic immunocytochemistry using subtype-specific antibodies. J Neurosci 14:3351–3363. Medline

Humphries MD, Prescott TJ (2010) The ventral basal ganglia, a selection mechanism at the crossroads of space, strategy, and reward. Prog Neurobiol 90:385–417. CrossRef Medline

Jones SR, O'Dell SJ, Marshall JF, Wightman RM (1996) Functional and anatomical evidence for different dopamine dynamics in the core and shell of the nucleus accumbens in slices of rat brain. Synapse 23:224–231. CrossRef Medline

Kelley AE (2004) Memory and addiction: shared neural circuitry and molecular mechanisms. Neuron 44:161–179. CrossRef Medline

Kharkwal G, Brami-Cherrier K, Lizardi-Ortiz JE, Nelson AB, Ramos M, Del Barrio D, Sulzer D, Kreitzer AC, Borrelli E (2016) Parkinsonism driven by antipsychotics originates from dopaminergic control of striatal cholinergic interneurons. Neuron 91:67–78. CrossRef Medline

Lavín A, Grace AA (1994) Modulation of dorsal thalamic cell activity by the ventral pallidum: its role in the regulation of thalamocortical activity by the basal ganglia. Synapse 18:104–127. CrossRef Medline

Lin JY (2011) A user's guide to channelrhodopsin variants: features, limitations and future developments. Exp Physiol 96:19–25. CrossRef Medline

Lin JY, Lin MZ, Steinbach P, Tsien RY (2009) Characterization of engineered channelrhodopsin variants with improved properties and kinetics. Biophys J 96:1803–1814. CrossRef Medline

Lu XY, Ghasemzadeh MB, Kalivas PW (1998) Expression of D1 receptor, D2 receptor, substance P and enkephalin messenger RNAs in the neurons projecting from the nucleus accumbens. Neuroscience 82:767–780. Medline

Maina FK, Mathews TA (2010) A functional fast scan cyclic voltammetry assay to characterize dopamine D2 and D3 autoreceptors in the mouse striatum. ACS Chem Neurosci 1:450–462. CrossRef Medline

Mamaligas AA, Ford CP (2016) Spontaneous synaptic activation of muscarinic receptors by striatal cholinergic neuron firing. Neuron 91:574–586. CrossRef Medline

McBride WJ, Murphy JM, Ikemoto S (1999) Localization of brain reinforcement mechanisms: intracranial self-administration and intracranial place-conditioning studies. Behav Brain Res 101:129–152. CrossRef Medline

Mogenson GJ, Swanson LW, Wu M (1985) Evidence that projections from substantia innominata to zona incerta and mesencephalic locomotor region contribute to locomotor activity. Brain Res 334:65–76. CrossRef Medline

O'Neill B, Patel JC, Rice ME (2017) Characterization of optically and electrically evoked dopamine release in striatal slices from digenic knock-in mice with DAT-driven expression of channelrhodopsin. ACS Chem Neurosci 8:310–319. CrossRef Medline

Patel JC, Rossignol E, Rice ME, Machold RP (2012) Opposing regulation of dopaminergic activity and exploratory motor behavior by forebrain and brainstem cholinergic circuits. Nat Commun 3:1172. CrossRef Medline

Pennartz CM, Groenewegen HJ, Lopes da Silva FH (1994) The nucleus accumbens as a complex of functionally distinct neuronal ensembles: an integration of behavioural, electrophysiological and anatomical data. Prog Neurobiol 42:719–761. CrossRef Medline

Phillips PE, Hancock PJ, Stamford JA (2002) Time window of autoreceptor-mediated inhibition of limbic and striatal dopamine release. Synapse 44:15–22. CrossRef Medline

Quinn DM (1987) Acetylcholinesterase: enzyme structure, reaction dynamics, and virtual transition-states. Chem Rev 87:955–979. CrossRef

Salinas AG, Davis MI, Lovinger DM, Mateo Y (2016) Dopamine dynamics and cocaine sensitivity differ between striosome and matrix compartments of the striatum. Neuropharmacology 108:275–283. CrossRef Medline

Sesack SR, Aoki C, Pickel VM (1994) Ultrastructural localization of D2 receptor-like immunoreactivity in midbrain dopamine neurons and their striatal targets. J Neurosci 14:88–106. Medline

Shin JH, Adrover MF, Wess J, Alvarez VA (2015) Muscarinic regulation of dopamine and glutamate transmission in the nucleus accumbens. Proc Natl Acad Sci U S A 112:8124–8129. CrossRef Medline

Sulzer D, Cragg SJ, Rice ME (2016) Striatal dopamine neurotransmission: regulation of release and uptake. Basal Ganglia 6:123–148. CrossRef Medline

Tanda G, Valentini V, De Luca MA, Perra V, Serra GP, Di Chiara G (2015) A systematic microdialysis study of dopamine transmission in the accumbens shell/core and prefrontal cortex after acute antipsychotics. Psychopharmacology 232:1427–1440. CrossRef Medline

Threlfell S, Clements MA, Khodai T, Pienaar IS, Exley R, Wess J, Cragg SJ (2010) Striatal muscarinic receptors promote activity dependence of dopamine transmission via distinct receptor subtypes on cholinergic interneurons in ventral versus dorsal striatum. J Neurosci 30:3398–3408. CrossRef Medline

Threlfell S, Lalic T, Platt NJ, Jennings KA, Deisseroth K, Cragg SJ (2012) Striatal dopamine release is triggered by synchronized activity in cholinergic interneurons. Neuron 75:58–64. CrossRef Medline

Trout SJ, Kruk ZL (1992) Differences in evoked dopamine efflux in rat caudate putamen, nucleus accumbens and tuberculum olfactorium in the absence of uptake inhibition: influence of autoreceptors. Br J Pharmacol 106:452–458. CrossRef Medline

Voorn P, Brady LS, Schotte A, Berendse HW, Richfield EK (1994) Evidence for two neurochemical divisions in the human nucleus accumbens. Eur J Neurosci 6:1913–1916. CrossRef Medline

Wang L, Zhang X, Xu H, Zhou L, Jiao R, Liu W, Zhu F, Kang X, Liu B, Teng S, Wu Q, Li M, Dou H, Zuo P, Wang C, Wang S, Zhou Z (2014) Temporal components of cholinergic terminal to dopaminergic terminal transmission in dorsal striatum slices of mice. J Physiol 592:3559–3576. CrossRef Medline

Weiner DM, Levey AI, Brann MR (1990) Expression of muscarinic acetylcholine and dopamine receptor mRNAs in rat basal ganglia. Proc Natl Acad Sci U S A 87:7050–7054. CrossRef Medline

West EA, Carelli RM (2016) Nucleus accumbens core and shell differentially encode reward-associated cues after reinforcer devaluation. J Neurosci 36:1128–1139. CrossRef Medline

Wieczorek W, Kruk ZL (1995) Influences of neuronal uptake and D2 autoreceptors on regulation of extracellular dopamine in the core, shell and rostral pole of the rat nucleus accumbens. Brain Res 699:171–182. CrossRef Medline

Wise RA (2004) Dopamine, learning and motivation. Nat Rev Neurosci 5:483–494. Medline

Yan Z, Surmeier DJ (1996) Muscarinic (m2/m4) receptors reduce N- and P-type Ca2+ currents in rat neostriatal cholinergic interneurons through a fast, membrane-delimited, G-protein pathway. J Neurosci 16:2592–2604. Medline

Yan Z, Song WJ, Surmeier J (1997) D2 dopamine receptors reduce N-type Ca2+ currents in rat neostriatal cholinergic interneurons through a membrane-delimited, protein-kinase-C-insensitive pathway. J Neurophysiol 77:1003–1015. Medline

Yang CR, Mogenson GJ (1987) Hippocampal signal transmission to the pedunculopontine nucleus and its regulation by dopamine D2 receptors in the nucleus accumbens: an electrophysiological and behavioural study. Neuroscience 23:1041–1055. CrossRef Medline

Záborszky L, Alheid GF, Beinfeld MC, Eiden LE, Heimer L, Palkovits M (1985) Cholecystokinin innervation of the ventral striatum: a morphological and radioimmunological study. Neuroscience 14:427–453. CrossRef Medline

Zhang L, Zhou FM, Dani JA (2004) Cholinergic drugs for Alzheimer's disease enhance in vitro dopamine release. Mol Pharmacol 66:538–544. CrossRef Medline

Zhang S, Qi J, Li X, Wang HL, Britt JP, Hoffman AF, Bonci A, Lupica CR, Morales M (2015) Dopaminergic and glutamatergic microdomains in a subset of rodent mesoaccumbens axons. Nat Neurosci 18:386–392. CrossRef Medline

Zhou L, Furuta T, Kaneko T (2003) Chemical organization of projection neurons in the rat accumbens nucleus and olfactory tubercle. Neuroscience 120:783–798. CrossRef Medline